JOURNAL OF CATALYSIS 27, 343–356 (1972)

Equilibria of Decomposition Reactions of Carbon Monoxide and Methane over Nickel Catalysts

JENS R. ROSTRUP-NIELSEN

Haldor Topsøe Research Laboratories, P. O. Box 49, DK-2950 Vedbæk, Denmark

Received March 3, 1972

The equilibria of the decomposition reactions of carbon monoxide and methane were studied in the temperature range 450–700°C on various nickel catalysts by means of a thermogravimetric apparatus. As previously, equilibrium constants were obtained which imply deviations from constants based on graphite data. The equilibrium constants varied from catalyst to catalyst and were correlated with nickel crystallite size. Examination in the electron microscope showed a whisker-like structure of the carbon formed, and that the diameter of the whisker was very close to that of the nickel crystallite attached to it. Deviations from graphite data may be explained by a disordered structure of the carbon and by a higher surface energy depending on the whisker diameter. The chemical composition and the activity of the catalyst appeared to be of minor importance for the deviations from graphite data. The reactions were prevented by sulfur chemisorbed on the nickel surface.

INTRODUCTION

It is well known that coking of catalysts for steam naphtha reforming may take place in two ways. First, coke may be formed due to poor activity or selectivity of the catalyst for conversion of naphtha to gaseous products, i.e., hydrogen, carbon monoxide, carbon dioxide, and methane. The carbonaceous deposits may be stable in a steady state condition even if the equilibrium composition predicts no formation of carbon. Secondly, carbon may be formed from the products carbon monoxide and methane when the equilibrium composition shows positive affinity for decomposition of these components. The present work, being part of a study on coking of naphtha-reforming catalysts, deals with decomposition of carbon monoxide, i.e., the Boudouard reaction, and with decomposition of methane:

$$2CO = C + CO_2 + 41.2\ \text{kcal}; \quad (1)$$

$$CH_4 = C + 2H_2 - 17.6\ \text{kcal}. \quad (2)$$

Normally, coking originating from these reactions is eliminated by operating with an excess of steam so that thermodynamics predict no formation of carbon after establishment of equilibrium. However, early studies by Dent (*1*) revealed that the Boudouard equilibrium was influenced by the carbon modification involved. Later, Dent *et al.* (*2*) studied the equilibria of both reactions on a nickel catalyst. Both reactions showed equilibrium constants deviating from those based on graphite data, implying that higher contents of carbon monoxide and methane, respectively, were allowed before coking was observed. The results indicated formation of nonideal graphite. Later, Nicklin and Whittaker (*3*) reported equilibrium constants for other catalysts showing extremely high deviations from graphite values when urania is present in the catalyst. On this basis the present study of the two reactions was performed over a wide range of nickel catalysts to elucidate the influence on the observed nonideal equilibrium constant of various catalyst parameters.

Chemisorption studies of carbon monoxide have shown results varying from catalyst to catalyst. This was previously explained by an influence of the carrier on the chemisorption properties of the metal due to the electronic properties of the junction metal/support (*4*), whereas more recent studies (*5*, *6*) favor an explanation in terms of different amounts of specific nickel sites from catalyst to catalyst.

The formation of carbon by the Boudouard reaction on monocrystalline nickel was studied at 550°C by Leidheiser and Gwathmey (*7*, *8*), who found a strong influence of crystal orientation. Carbon was found on the (111) faces, whereas no carbon was detected on the (100) and (110) faces. Gwathmey (*9*) also studied the influence on the reaction of the *d*-character of the metal, using copper–nickel alloys. Again, carbon was formed selectively on the (111) faces, indicating that the properties of the individual surface atom and its neighbors are more important for the reaction than are the electronic properties of the bulk phase.

The surface structure of carbon on nickel has been studied recently by Coad and Rivière (*10*) using Auger spectroscopy. Two structures were observed and attributed to nickel carbide (Ni_3C) and to graphite on the surface. On heating above about 400°C the carbide decomposed, forming graphite. This is in accordance with bulk chemistry, nickel carbide being unstable between about 400 and 1600°C. In this temperature range carbon is dissolved to a small extent in nickel (*11*). A similar result was obtained by magnetic studies by Escoubes and Eyraud (*12*) in a study of the Boudouard reaction. Above 350°C no modification of the magnetic properties of nickel was detected. The existence of an intermediate carbide phase during the Boudouard reaction at temperatures above 400°C has been discussed by Renshaw, Roscoe, and Walker (*13*). However, the existence of a precursor for carbon in the form of an intermediate carbide or some carbon dissolved in nickel would not change the equilibrium constant.

Examination in an electron microscope of the carbon product indicated that it was very porous and consisted of "tangled threadlike segments" (*8*); Hofer, Sterling, and McCartney (*14*) found that many of the whisker-like threads appeared to be tubules. They assumed that the tubules were not hollow, but contained material less dense than the outside walls. Most of the threads contained nickel nuclei of about the same diameter as that of the corresponding thread. The nuclei appeared almost invariably at the ends of the threads. Renshaw, Roscoe, and Walker (*13*) observed this structure and a flake-like material as well.

Two different structures were also reported by Robertson (*15*), who studied the decomposition of methane at 750°C on nickel films. The two types of deposit were identified as "flake" and "polycrystalline." The "flake"-carbon showed a perfect crystalline graphite nature whereas fibrous polycrystalline carbon showed a disordered structure containing nickel particles similar to that observed in carbon formed by decomposition of carbon monoxide. However, some degree of graphitic order was indicated, as the basal planes (0001) of the crystallites were in a preferred orientation parallel to the long axis of the fiber. These results were confirmed by Baird *et al.* (*16*), who also observed the basal graphite planes to be parallel with the surface of the metal particle, but the structure showed no preference of direction of growth. The fibers were surrounded by an amorphous layer.

The component to be decomposed appears to be of minor importance for the structure of the carbonaceous deposits. LEED studies by Edmonds and Pitkethly (*17*, *18*) indicated that the structure of carbon formed by decomposition of carbon monoxide is very close to that formed in LEED studies involving cracking of ethylene. It has been claimed (*19*), also on basis of LEED studies, that similar structures of carbon are observed from decomposition of methane and ethylene. The similarities between structures obtained from methane and other hydrocarbons have also been discussed by Walker *et al.* (*13*) and Baird *et al.* (*16*).

METHODS

Apparatus

The experiments were carried out in a thermogravimetric system (Fig. 1). The catalyst was placed in a basket hung in a

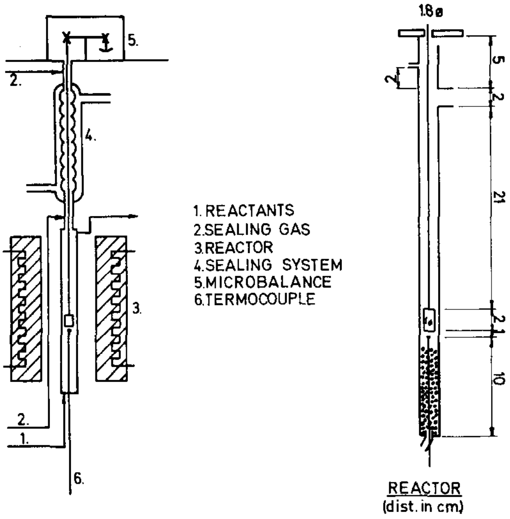

FIG. 1. Apparatus for coking studies.

REEC-EMB1 electro-microbalance having a recorder output sensitivity of 100 mV/mg. Weight changes of 0.1 mg could be observed. The basket was placed in a reactor surrounded by an electrically heated furnace. The reactor and the microbalance were separated by a nitrogen sealing system.

The basket was made of gold (14 carat covered by 18 carat). For experiments above 600°C a basket of inconel was used. The walls of the basket were perforated by holes with a diameter of approx. 1.2 mm. The reactor was made of inconel. CO and CO_2, or H_2 and CH_4, were introduced through capillary flowmeters to the bottom of the reactor, and left the system at the reactor top together with the sealing gas. Calculations showed back-diffusion of N_2 to have a negligible effect on the gas composition over the catalyst.

Measurements of axial temperature profiles in the empty reactor indicated temperature gradients of less than 2°C in the basket zone. During the experiment, the temperature was measured just below the basket. The mean temperature in the catalyst was 1–2°C higher than measured. The temperature was adjusted by means of a thyristor controller.

Gases

All gases were taken from cylinders. CO and CO_2 were used unpurified. Gas-chromatographic analyses indicated impurities (mainly N_2) to be less than 1%. N_2 and H_2 were purified over Cu wire at 250–275°C. CH_4 was taken unpurified from a cylinder. Gas-chromatographic analyses indicated impurities of N_2 and CO_2 of 1.4 and 0.7 vol %, respectively. A minor content of C_2H_4 (0.02 vol %) was found, but no traces of higher hydrocarbons were detected. A few experiments including removal of CO_2 over ascarite showed this to be of no importance. With no purification CO_2 passed unconverted through the reactor.

Catalysts

The catalysts, most of which were based on magnesia (A-types) are described in Table 1. The samples of preparations include examples of sulfur poisoning, various reduction procedures, sintering, and coking. Moreover, the nickel content was changed, and cobalt and copper were introduced. Other catalysts (types B–D) were prepared by impregnation on various commercial carriers such as magnesium aluminium spinel, η-alumina (Pechiney Saint Gobain SAS-350), and α-alumina (Carl Otto). Some of the catalysts were promoted with alkali. One catalyst was promoted with urania following the preparation technique described by Nicklin *et al.* (*3*) in relation to their studies of the Boudouard reaction.

The catalysts were reduced in hydrogen at 850°C for a period of 2 hr, unless otherwise stated. The content of nickel in the reduced state was determined by chemical analysis involving selective dissolving of nickel metal by treatment with a bromine–methanol solution.

The nickel area was expressed as the sulfur capacity, using a method described previously (*20*). Cobalt and copper were assumed to chemisorb sulfur as does nickel. On the basis of the analysis of reduced nickel and the sulfur capacity, a mean radius of the nickel crystallites was calculated by the formula:

$$r_{\text{mean}} = 1.48 \times 10^4 \, (x_{\text{Ni}}/s_0)\text{A}, \qquad (3)$$

where x_{Ni} = reduced nickel (wt %), and s_0 = sulfur capacity (wt ppm). The formula

TABLE 1
CATALYST PROPERTIES

Catalyst no.	Comments	Content of reduced Ni (wt %)	Ni-area (expressed as S-capacity) (ppm S)	Particle size: Calc. r_{mean} (Å)	Particle size: Electron microscope particle diameter (Å)	Activity C_2H_6 conversion (%)
A-types, fixed chemical composition (25% Ni)						
A1		23.8	885	398	250–2500	12
A2	A1, S-poisoned: 760 ppm S	25.2	760	490	500–4000	<1
A3	Reduced in excess dry H_2, 2 hr	16.4	4100	59	50–250	44
A4	A3, reduced in $H_2O/H_2 = 3$, 16 hr	23.1	1670	205	500–1000	28
A5	6 wt % C	6.4	(525)	(179)	100–1500	
A6	A5, regenerated	19.5	980	293	100–750	
A7	Sintered	23.5	470	740	150–2000	2.4
A-types, modified composition						
A8	29% Ni	27.6	3400	120	75–400	59
A9	19% Ni	18.9	2580	109	75–400	
A10	14% Ni	13.9	1844	112	50–125	58
A11	11% Ni	9.1	1880	85	50–200	
A12	6% Ni	5.0	1110	67	50–200	
A13	Ni/Cu = 0.7/1.3	7.6	545	206	50–150	<1
A14	Co replacing Ni	22.9[a]	2420	140	–(500)	<1
B-types						
B1		8.0	195	607	500–2500	
B2		12.4	246	745	–2000	8.5
B3	1.60 wt % K	16.6	878	282	500–2500	
B4	1.53 wt % K	17.5	390	665	–2000	0.26
C-types						
C1		16.5	2840	86	100–400	23
C8	1.65 wt % K	11.5	2800	61	50–250	<1
D-type						
D1	10.0 wt % U, 0.07 wt % K	13.7	1400	147	–1000	

[a] Percent red. Co.

is derived assuming the nickel crystallites to be half-spheres exposing the spherical surface, the saturated surface being assumed to contain 44.2×10^{-9} g S/cm^2. The distribution of nickel crystallite sizes was examined by means of an electron microscope.

The catalyst activity was estimated from experiments on the steam reforming of ethane. The figures are conversions obtained at standard conditions (500°C; 1 atm; $H_2O/C_2H_6 = 8$ mole/mole; space velocity $= 42 \times 10^3$ vol C_2H_6/vol catalyst hr; catalyst particle size = 0.1–0.3 mm). Although this way of comparing catalyst activities may be doubtful, it is sufficient for the present study in serving as a rough classification of the catalysts.

Procedure

A sample of reduced catalyst as 2–3 mm particles was placed in the basket. A catalyst bed length of 10 mm (volume 0.79 ml) was used provided the catalyst weight did not exceed 0.72 g. The catalyst was heated in H_2 (4 nliter/hr) until temperature and sample weight had stabilized. When studying the Boudouard reaction, H_2 was removed by purging with N_2 (4 nliter/hr) for a period of 5 min. N_2 was replaced by CO_2 (10 nliter/hr) and immediately after that, CO was added. The CO flow was increased stepwise at intervals of 5–10 min until an increase in weight was indicated on the recorder. Then, the CO flow was decreased stepwise, until a decrease in weight was indicated. By interpolation, the CO concentration corresponding to a stable weight of the catalyst was found. This was defined as the equilibrium state. In several experiments this procedure was repeated and no hysteresis effects were observed. The experiments on methane decomposition followed a similar procedure, CH_4 being added stepwise to H_2.

A certain excess of CO or CH_4 was required to start the reaction. This supersaturation was reproduced in experiments including two coking–decoking cycles, whereas reproduction from experiment to experiment was poor. When heating catalyst A1 in pure CO and CH_4 at a rate of 4°C/min, carbon formation was detected at 280 and 230°C, respectively.

RESULTS AND DISCUSSION

Electron Microscopy

Catalyst samples exposed to pure carbon monoxide or methane at 500°C were examined in an electron microscope. Whisker-like structures as shown in Fig. 2 were observed, whereas no flake-like material was identified. The whiskers had the same tubular appearance as that described by Hofer *et al.* (*14*). Similar structures were observed on samples exposed to naphtha. Most of the whiskers contained a nickel crystallite, normally located at the end, and the diameter of the whisker was very close to that of the nickel crystallite. This observation is important for the interpretation of the equilibrium studies and will be discussed in more detail.

The preferred orientations (i.e., the basal graphitic planes parallel to the long axis of the fiber) observed by Robertson and Baird (*15*, *16*) reflect an unusual growth habit as the growth of whiskers normally leads to single crystals in which the whisker axis coincides with a low index crystallographic direction (i.e., the <0001> direction). The normal growth may be explained by assuming the presence of an axial screw dislocation. However, Sears (*21*) has demonstrated that for graphite, in a certain region of supersaturation, it may be possible to obtain a whisker with its axis parallel to the *c*-plane (0001). First, a short whisker is formed by the normal mechanism with coincident *c*-axis and whisker-axis. Then a preferential two-dimensional nucleation of *c*-layers [(0001)-planes] occurs on the columnar *a*-surfaces. The *c*-layer grows around the parent core whisker. The growth of one layer over the other would form the configuration of a radial edge dislocation providing a scroll whisker. Sears' calculations may account for the preferred orientations observed by Robertson and Baird, and probably for the tubular appearance observed by Hofer *et al.* (*14*) and in the present work, as the less dense center could be the core whisker.

Coking studies performed in the electron microscope showed some interesting results. When heating catalyst samples in the electron microscope, residual oil originating from the equipment cracked on the catalyst. The whisker growth started on the smallest crystallites. The growth appeared spontaneous. The growth on larger crystals started later. The smallest crystallites may be more reactive as they show to a greater extent surface irregularities at which decomposition might most easily occur. The importance of such sites for the *rate* of the Boudouard reaction has been emphasized by Gwathmey (*9*) and Grenga (*22*).

The whiskers formed in the electron

FIG. 2. Electron micrograph of whisker-like carbon formed by decomposition of CH_4 on catalyst B1 at 500°C.

microscope were very thin with no dependence on nickel particle size. This could be the core whisker reflecting that the supersaturation at the specific conditions has not allowed formation of a scroll whisker. Similar thin whiskers with a diameter much less than that of the metal particle were observed in Pfefferkorn's studies of oxidation of metals (*23*).

A mechanism resulting in scroll whiskers having a diameter close to that of the nickel particle has not yet been formulated. It should be noticed from Fig. 2 that the core whiskers appear to grow from an edge of the nickel crystallites. The scroll whisker might be assumed to grow from the core whisker in the direction of the nickel crystallite, as most likely the reaction takes place at the interface of carbon and nickel (*12*).

Equilibrium Studies

CO Decomposition. The experimental results are shown in Tables 2–4. Equilibrium constants have been calculated from:

$$K_p = (CO_2)/[(CO)^2 \cdot P]\ \text{atm}^{-1}. \quad (4)$$

Moreover, calculations have been made of deviation of the free energy, ΔG_c, from that involved in the reaction with graphite. This value reflects the excess energy of the carbon formed compared to that of graphite:

$$\Delta G_c = \Delta G^\circ_{\text{actual reaction}} - \Delta G^\circ_{\text{graphite reaction}}; \quad (5)$$

$$\Delta G_c = -RT \ln K_{p_{\text{observed}}} + RT \ln K_{p_{\text{graphite}}}. \quad (6)$$

Experiments with catalyst A1 at various

TABLE 2

CO DECOMPOSITION: EXPERIMENTS WITH CATALYST A1 AT VARIOUS TEMPERATURES

Exp. no.	Temp. (°C)	CO vol % Start of coke formation	CO vol % Equil. completed	Pressure (mm Hg)	$K_{p_{\text{observed}}}$ (atm^{-1})	$K_{p_{\text{graphite data}}}$ (atm^{-1})	ΔG_c (kcal/mole)
513[a]	450	8.27	5.65	764	294	1457	2.30
322[a]	500	28.6	12.3	760	58.0	227	2.09
714	500	15.3	11.5	766	66.5	227	1.89
719	500	25.9	13.8	764	45.0	227	2.48
514[a]	550	44.4	21.6	767	16.6	44.6	1.61
323[a]	600	69.7	33.3	761	6.00	10.6	0.97
330	700	69.7	68.0	769	0.684	0.934	0.60

[a] Two or more cycles performed.

temperatures (Table 2) show results broadly in line with those obtained by Dent (*2*). As the free energy of the carbon formed is higher (1–2 kcal/mole) than that of graphite, higher contents of carbon monoxide are observed in the equilibrium state. The deviations from graphite data diminish at higher temperature. From Fig. 3, the heat of reaction is estimated as 32 kcal/mole in the temperature range studied (450–600°C), whereas the corresponding value based on graphite is 41 kcal/mole. Estimates of the entropy of reaction show values higher than those based on graphite, indicating a more disordered structure.

Experiments with various catalysts reveal a great influence on the equilibrium constant from the catalyst type (Tables 3 and 4). At 500°C, the excess free energies, ΔG_c, vary from 1.56 to 3.75 kcal/mole, whereas at 600°C lower values are found, 0.97–2.69 kcal/mole. The data of Dent (*2*) are within these ranges, whereas Nicklin's results on urania-promoted catalyst (*3*) yield much higher energies. However, catalyst D1 prepared in accordance with Nicklin, shows ΔG_c in the lower part of the range indicating no specific function of urania. In general, examination of the results indicates the chemical composition of the catalyst to be of minor importance. Thus, addition of alkali to the catalysts has caused no significant changes of the equilibrium constant. On the other hand, among

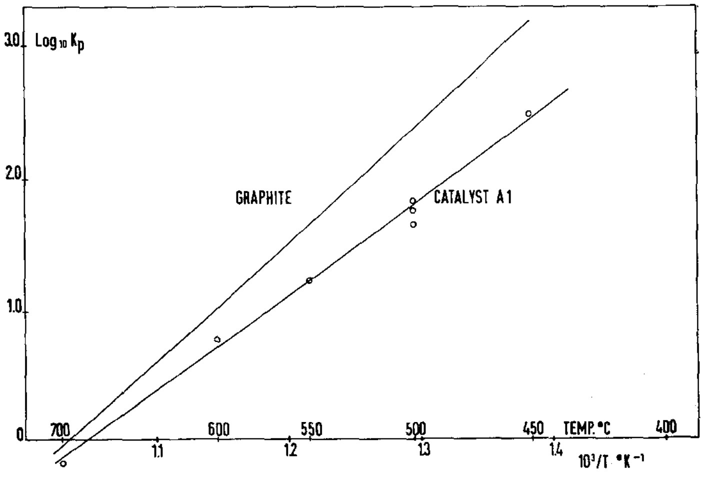

FIG. 3. CO decomposition on catalyst A1. Temperature dependence of equilibrium constant.

TABLE 3
CO DECOMPOSITION: EXPERIMENTS AT 500°C WITH VARIOUS CATALYSTS

Catalyst no.	Max. part. size (Å)	Exp. no.	CO vol %		Pressure (mm Hg)	K_p (atm^{-1})	ΔG_c (kcal/mole)
			Start of coke formation	Equil. completed			
A-types							
A1	2500	322	28.6	12.3	760	58.0	2.09
A1		714	15.3	11.5	766	66.5	1.89
A1		715	25.9	13.8	764	45.0	2.48
A2	(4000)	511	(60)	56	770	(1.4)	(7.8)
A3	250	421[a]	31.1	14.0	770	43.3	2.54
A3		802	15.3	14.5	763	40.6	2.64
A4	1000	419[a]	18.4	12.3	766	57.6	2.11
A5	1500	526[a]	18.7	12.7	760	54.1	2.20
A6	750	527	29.6	13.8	757	45.5	2.47
A7	2000	603	20.0	12.7	767	53.8	2.21
A8	400	809	15.3	13.8	765	45.0	2.48
A9	400	810	15.3	14.6	760	40.1	2.66
A10	125	506[a]	37.2	20.0	771	19.7	3.75
A11	200	812	29.6	16.7	755	29.9	3.11
A12	200	811	15.3	15.3	757	38.6	2.72
A12		813	15.3	13.8	760	45.2	2.48
A13	(150)	601	67.7	18.6	770	23.2	3.50
A14	(500)	602	33.3	12.7	770	53.5	2.22
Other types							
B1	2500	428[a]	31.1	11.3	761	63.5	1.96
B2	2000	721	12.3	10.4	764	82.4	1.56
B2		727	15.3	11.0	768	72.8	1.74
B3	2500	503[a]	31.1	12.3	767	57.5	2.11
B3		722	15.3	13.8	762	45.1	2.48
B3		726	18.7	12.3	764	57.7	2.10
B4	2000	728	12.3	11.5	766	66.5	1.89
C1	400	401[a]	33.3	20.0	760	20.0	3.73
C2	250	405[a]	42.8	19.2	759	21.9	3.59
C2		804	29.6	20.0		20.1	3.72
D1	1000	720	15.3	11.5	764	66.5	1.89
Dent (*2*)				11.0	(760)	73.5	1.73
Nicklin (*3*)				41.2	(760)	1.2	8.02
Graphite data				6.4	(760)	22.7	0

[a] Two or more cycles performed.

A-types, great variations are observed. Even the reduction procedure and sintering of the catalyst may influence the results. Catalyst activity appears to play no role.

The sulfur-poisoned catalyst A2 does not follow the general trend. It was difficult to conclude whether carbon formation occurred. This is in line with the observations made by Sickafus (*24*) who studied the influence of chemisorbed sulfur on the adsorption of carbon on nickel by means of Auger spectroscopy. The experiments demonstrated that adsorbed carbon does not overlap into the sulfur domains. Therefore, it was assumed that the carbon is limited to the regions that are not already occupied by sulfur. Earlier observations of Crell *et al.* (*25*) showed chemisorption of carbon

TABLE 4
CO DECOMPOSITION: EXPERIMENTS AT 600°C WITH VARIOUS CATALYSTS

Catalyst no.	Max. particle size (Å)	Exp. no.	CO vol % Start of coke formation	CO vol % Equil. completed	Pressure (mm Hg)	K_p (atm^{-1})	ΔG_c (kcal/mole)
A-types							
A1	2500	323	69.7	33.3	761	6.00	0.97
A3	250	422[a]	63.0	50.0	770	1.98	2.89
A4	1000	420[a]	56.4	44.4	765	2.81	2.28
A10	125	510	69.7	48.2	768	2.22	2.69
Other types							
B1	2500	429[a]	66.7	35.5	756	5.14	1.23
B3	2500	430[a]	52.4	35.5	767	5.08	1.25
B3		505[a]	52.4	33.3	769	5.93	0.99
C1	400	402[a]	69.7	49.9	756	2.02	2.85
C2	250	406[a]	69.7	43.4	760	3.01	2.16
Dent (*2*)				34.5	(760)	5.6	
Nicklin (*3*)				70.2	(760)	0.60	
Graphite Data				26.4	(760)	10.6	0

[a] Two or more cycles performed.

monoxide restricted to the empty places of the sulfur-poisoned surface. Crell's monolayer formed at low temperature has contained hydrogen from the dissociative chemisorption of hydrogen sulfide, and the results can be explained by chemisorption of carbon monoxide easily replacing hydrogen (*26*), whereas chemisorbed sulfur remains stable. As the monolayer of sulfur formed from hydrogen sulfide at temperatures above 200°C is a surface compound containing no hydrogen (*27*, *28*), no reaction of carbon monoxide is expected on a nickel catalyst covered with sulfur at high temperatures. The presence of coke deposits before the experiment in catalyst A5 had no influence.

As shown in Fig. 4, the equilibrium constant correlates with maximum nickel crystallite size (determined by an electron microscope). Correlation coefficients of 0.70 and 0.96 have been calculated on the basis of the data at 500 and 600°C, respectively, indicating great significance. The greatest deviation from graphite data is observed over catalysts with the smallest nickel crystallites. It should be noticed that A-types with nickel–copper alloy or cobalt as metal phase fit in the correlation indicating the bulk properties of the metal to be of less importance. This is in accord-

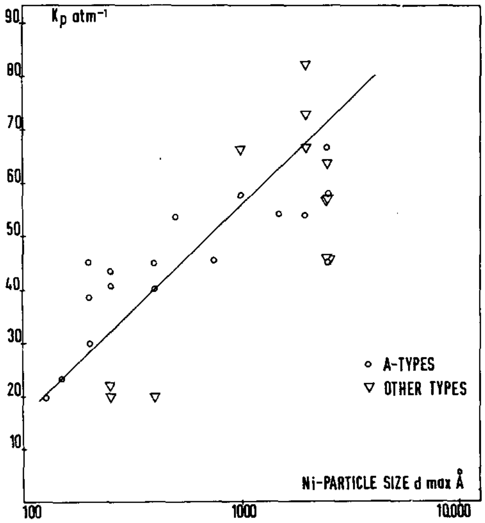

FIG. 4. CO decomposition on various catalysts at 500°C. Correlation of equilibrium constant and maximum diameter of nickel crystallites. K_p (graphite) = 227 atm^{-1}.

ance with the observations of Gwathmey (*9*).

On the basis of the observations in the electron microscope showing the diameter of the carbon whisker close to and not greater than that of the nickel crystallite, it appears reasonable to ascribe the effect of the particle size to being geometrical. The deviations from graphite data might be explained by a contribution of the surface energy. The surface energy increases with decreasing whisker diameter and nickel particle size. In a simplified model assuming the whisker to be an infinite cylinder, the Kelvin equation becomes:

$$\mu - \mu_0 = \gamma \cdot M/r \cdot \rho, \tag{7}$$

where μ and μ_0 are free energies of a cylinder with radius r and of carbon with no curvature, respectively. γ is the surface tension, and M and ρ are molecular weight and density, respectively. The deviation from graphite data, ΔG_c, may be expressed by:

$$\Delta G_c = \mu - \mu_0 + \mu^*, \tag{8}$$

where μ^* is the contribution from structural defects compared to graphite. Inserting (7) in (8) yields:

$$\Delta G_c = (\gamma \cdot M/\rho) \cdot (1/r) + \mu^*; \tag{9}$$

$$\Delta G_c = k \cdot (1/r) + \mu^*. \tag{10}$$

When ΔG_c is plotted as function of $(1/r)$, a straight line is obtained.

Some difficulties arise when applying this model to correlate ΔG_c with nickel particle size. First, every catalyst displays a broad range of nickel crystallite sizes. In principle, the equilibrium should be established first over the largest crystallites forming carbon with smaller energy. However, when few large crystallites are present, the results may well reflect the equilibrium over a smaller crystallite size because of the sensitivity of the balance. Secondly, the supersaturation required to start the reaction might result in coking on smaller crystallites as well. This is likely, as the observations in the electron microscope indicated the reaction to start on small crystallites, and it may bias the results. Thirdly, as mentioned above, whiskers with diameter less than that of the nickel crystallite may be formed. These effects all imply whiskers with smaller diameter than that of the maximum nickel particle size which, consequently, may not be the correct but the most appropriate parameter for the correlations. Therefore, any strict use of ΔG_c is ambiguous.

These problems and accumulated uncertainties from the experiments are reflected in the plot shown in Fig. 5. By linear regression analysis the slope was determined with a relative error of 10–15%. Using a density for the whisker of 2 g/ml, the surface tension, γ, is estimated as 7900 erg/cm^2. The same result is obtained from the data at 600°C (Fig. 6). In the literature, γ for a nonbasal surface is estimated to be 4000–6300 erg/cm^2 (*29*, *30*). It is doubtful to compare these values with the experimental results as, according to Baird (*16*), the carbon structure at the whisker surface appears very disordered. Moreover, the systematic effects mentioned above result in too-high estimates of the surface tension. However, on the basis of the observed correlation it appears reasonable to ascribe changes in equilibrium constant

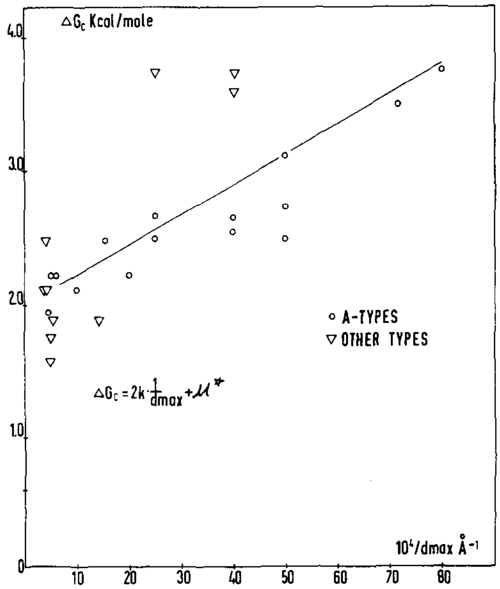

FIG. 5. CO decomposition on various catalysts at 500°C. Deviation from graphite data and nickel crystallite size.

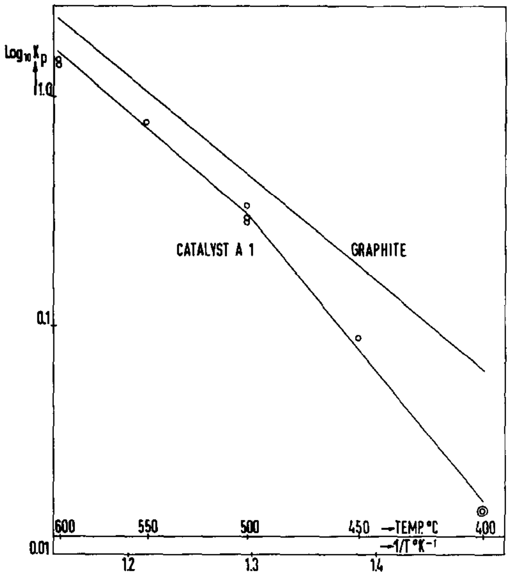

FIG. 6. CO decomposition on various catalysts at 600°C. Deviation from graphite data and nickel crystallite size.

from catalyst to catalyst to various surface energies of the carbon determined by the nickel crystallite size.

The value of μ^* is estimated to be 2 and 1.4 kcal/mole at 500 and 600°C, respectively, indicating the nonideal structure of the carbon deposits. This is supported by the observation in the electron microscope.

CH_4 Decomposition. The experimental results are shown in Tables 5 and 6. Equilibrium constants have been calculated from:

$$K_P = [(H_2)^2 \cdot P]/(CH_4) \text{ atm.} \qquad (11)$$

The excess free energy, ΔG_c, was calculated from Eq. (6).

Results from experiments with catalyst A1 at various temperatures are shown in Table 5. Contrary to what was obtained by Dent (*2*), ΔG_c deviates from the values calculated from the experiments with carbon monoxide, the deviation being less than previously. ΔG_c diminishes with increasing temperature, as shown previously. As shown in Fig. 7, the heat of reaction changes from −25 to −18 kcal/mole, the latter value being close to what is obtained on the basis of graphite data.

Experiments with various catalysts at 500°C showed trends similar to experiments with carbon monoxide. The results are shown in Table 6, indicating how the equilibrium constant correlates with maximum

TABLE 5

CH_4 DECOMPOSITION; EXPERIMENTS WITH CATALYST A1 AT VARIOUS TEMPERATURES

		CH_4 vol %					
Exp. no.	Temp. (°C)	Start of coke formation	Equil. completed	Pressure (mm Hg)	$K_{p_{\text{observed}}}$ (atm)	$K_{p_{\text{graphite data}}}$ (atm)	ΔG_c (kcal/mole)
616	400	96.2	88.3	758	0.0155	0.0636	1.88
494[a]	400	94.9	88.3	761	0.0155	0.0636	1.88
614	450	88.3	75.0	760	0.0833	0.1826	1.13
611	500	77.7	56.5	760	0.335	0.4619	0.56
617	500	77.0	58.4	762	0.296	0.4619	0.68
495[a]	500	77.0	59.2	764	0.283	0.4619	0.75
610	550	60.0	42.8	762	0.764	1.0524	0.52
618	600	47.3	32.2	762	1.43	2.1957	0.74
496[a]	600	41.2	31.0	772	1.38	2.1957	0.80
Dent (*2*)							
	410		86.0	(705)[b]	0.0055	0.0785	3.53
	525		61.8	(750)[b]	0.214	0.6968	1.80

[a] CO_2 removed.

[b] N_2 as balance to total pressure 760 mm Hg.

TABLE 6

CH_4 DECOMPOSITION: EXPERIMENTS AT 500°C WITH VARIOUS CATALYSTS

Catalyst no.	Max. particle size (Å)	Exp. no.	CH_4 vol %		Pressure (mm Hg)	K_p (atm)	ΔG_c (kcal/mole)
			Start of coke formation	Equil. completed			
A-types							
A1	2500	611	77.7	56.5	760	0.335	0.56
A1		617	77.7	58.4	762	0.296	0.68
A2	(4000)	709	(100)	(99.4)	767	(0.4×10^{-4})	(14.5)
A3	250	623	79.0	66.7	761	0.166	1.57
A4	1000	622	81.1	59.1	754	0.286	0.73
A7	2000	707	77.0	60.5	772	0.254	0.92
A10	125	708	83.3	71.5	771	0.112	2.17
A13	(150)	625	96.2	91.5	760	0.0079	6.27
A13		497[a]	90.4	(90.4)	770	0.0103	5.84
A14	(500)	628	81.1	63.9	758	0.204	1.25
Other types							
B1	2000	706	75.0	55.0	769	0.364	0.366
B3	2500	702	85.8	61.3	763	0.243	0.986
C1	400	629	81.1	68.2	760	0.148	1.75
D1	1000	712	75.5	59.2	767	0.280	0.77
Dent (*2*) (interpolation)						(0.142)	(1.78)
Graphite data					760	0.4619	0

[a] CO_2 removed.

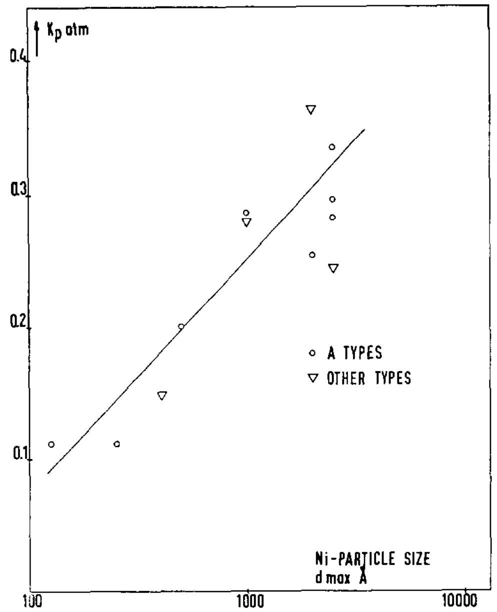

FIG. 7. CH_4 decomposition on catalyst A1. Temperature dependence of equilibrium constant.

nickel crystallite size. A correlation coefficient of 0.81 has been calculated indicating great significance.

It should be noticed that promotion with alkali or urania and use of cobalt have no detectable influence on the results. As previously, coking on sulfur-poisoned catalyst was unlikely. Contrary to the results with carbon monoxide, the nickel–copper catalyst (A13) does not follow the general trend, as ΔG_c is nearly 3 times higher than that of the nickel catalyst with smallest crystallites. In this connection it should be noticed that copper shows no chemisorption of methane or activity for exchange reactions (*31*), whereas carbon monoxide is chemisorbed on copper already at low temperature (*32*). However, additional investigations are required to explain the behavior of catalyst A13.

The surface tension of the whiskers is estimated from a correlation of excess free energies and reciprocals of maximum nickel

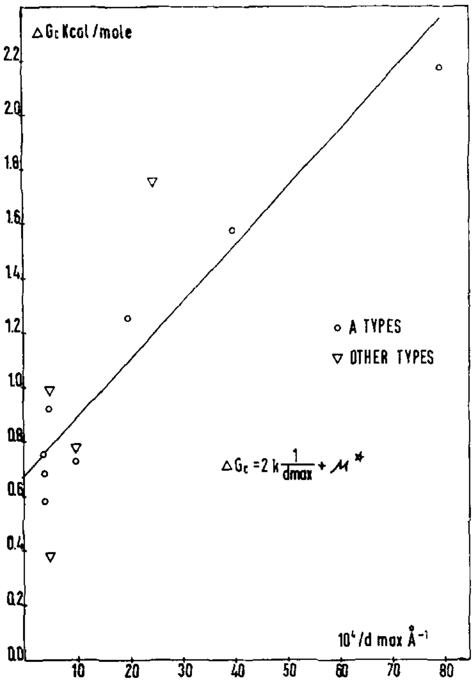

FIG. 8. CH_4 decomposition on various catalysts at 500°C. Deviation from graphite data and nickel crystallite size.

particle sizes as indicated in Fig. 8. By linear regression analysis the slope has been determined with a relative error of 18% and, based on this, the surface tension is estimated to be 7400 erg/cm^2, which is close to the result from the experiments with carbon monoxide (7900 erg/cm^2). Moreover, μ^* is 0.7 kcal/mole, which is less than that obtained with carbon monoxide (2 kcal/mole). In principle, this reflects that carbon formed by decomposition of methane may have a structure more ideal than that formed in the Boudouard reaction. The result might also be ascribed to a nonidentified systematic error introduced when studying the CH_4/H_2 system instead of the CO/CO_2 system.

CONCLUSIONS

The equilibrium constants of the decomposition reactions of carbon monoxide and methane are influenced by nickel catalysts resulting in higher concentrations of carbon monoxide and methane, respectively, in the gas phase at equilibrium. The equilibrium constant correlates with the maximum nickel crystallite size of the catalyst. Thus, the greatest deviations from graphite data are observed on catalysts with small nickel crystallites. The deviation from graphite data is explained by a more disordered structure of the carbon formed and by a contribution from the surface energy of the carbon whisker. The latter part changes from catalyst to catalyst, as the whisker diameter is related to the size of the nickel crystallites. This was confirmed by examination of the carbon structure in the electron microscope. The deviations from graphite data were less for the decomposition of methane than those observed for the decomposition of carbon monoxide.

The chemical composition of the catalysts appeared to have no influence on the observed equilibrium data. Thus use of various carriers, presence of other components such as coke, potassium, and urania, or replacement of nickel by cobalt, had no influence, whereas factors determining the nickel particle size such as activation procedure and sintering are of major importance.

The data obtained on a nickel-copper catalyst differed from the general trend in the methane decomposition experiments, whereas normal behavior was observed in the experiments with carbon monoxide. Sulfur chemisorbed on the nickel surface most likely prevents the decomposition reactions.

ACKNOWLEDGMENTS

I wish to thank Dr. Haldor Topsøe for permission to publish the results, and Mrs. U. Ebert Petersen, Mr. E. Højengaard, and many of my colleagues for assistance in performing the experiments.

REFERENCES

1. DENT, F. J., AND COBB, J. W., *J. Chem. Soc. London* **2**, 1903 (1929).
2. DENT, F. J., MOIGNARD, L. A., EASTWOOD, A. H., BLACKBURN, W. H., AND HEBDEN, D., *Trans. Inst. Gas Eng.* 1945–1946, p. 602.
3. NICKLIN, M. B. E., AND WHITTAKER, R. J., *I.G.E.J.* **8**, 15 (1968).
4. O'NEILL, C. E., AND YATES, D. C. J., *J. Phys. Chem.* **65**, 901 (1961).

5. VAN HARDEFELD, R., AND HARTOG, F., *4th Int. Congr. Catal., Moscow, 1968,* preprint 70.
6. BRADSHAW, A. M., AND PRITCHARD, J., *Surface Sci.* **17**, 372 (1969).
7. LEIDHEISER, H., JR., AND GWATHMEY, A. T., *J. Amer. Chem. Soc.* **70**, 1206 (1948).
8. KEHRER, V. J., AND LEIDHEISER, H., JR., *J. Phys. Chem.* **58**, 550 (1954).
9. COX, E., LAWLESS, K. R., AND GWATHMEY, A. T., *Actes Congr. Int. Catal. 2nd 1960* **2**, 1605 (1961).
10. COAD, J. P., AND RIVIÉRE, J. C., *Surface Sci.* **25**, 609 (1971).
11. LANDER, J. J., KERN, H. E., AND BEACH, A. L., *J. Appl. Phys.* **23**, 1305 (1952).
12. ESCOUBES, M., AND EYRAUD, C., *Bull. Soc. Chim. Fr.* no. 10, 1369 (1966).
13. RENSHAW, G. D., ROSCOE, C., AND WALKER, P. L., JR., *J. Catal.* **22**, 394 (1971).
14. HOFER, L. J. E., STERLING, E., AND MCCARTNEY, J. T., *J. Phys. Chem.* **59**, 1153 (1955).
15. ROBERTSON, S. D., *Carbon (Oxford)* **8**, 365 (1971).
16. BAIRD, T., FRYER, J. R., AND GRANT, B., *Nature (London)* **233**, 329 (1971).
17. EDMONDS, T., AND PITKETHLY, R. C., *Surface Sci.* **15**, 137 (1969).
18. EDMONDS, T. O., AND PITKETHLY, R. C., *Surface Sci.* **17**, 4509 (1969).
19. BERTOLINI, J. C., *in* Discussion at symposium "Chemisorption and Catalysis" London, 1970 (to be publ. in *J. Inst. Petrol.*).
19. BERTOLINI, J. C., *in* "Chemisorption and Catalysis," Institute Petroleum, London, 1971.
20. ROSTRUP-NIELSEN, J. R., *J. Catal.* **21**, 171 (1971).
21. SEARS, G. W., *J. Chem. Phys.* **31**, 358 (1959).
22. GRENGA, H. E., *Diss. Abstr.* **28**, 2789 (1968).
23. PFEFFERKORN, G., *Z. wiss Mikrosk.* **62**, 109 (1954).
24. SICKAFUS, E. N., *Surface Sci.* **19**, 181 (1970).
25. CRELL, W., HOBERT, H., AND KNAPPE, B., *Z. Chem.* **8**, 396 (1968).
26. LAPOUJOULADE, J., *J. Chim. Phys. Physicochim. Biol.* **68**, 73 (1971).
27. ROSTRUP-NIELSEN, J. R., *J. Catal.* **11**, 220 (1968).
28. PERDEREAU, M., AND OUDAR, J., *Surface Sci.* **20**, 80 (1970).
29. GIRIFALCO, L. A., AND LAD, R. A., *J. Chem. Phys.* **25**, 693 (1956).
30. BRUCE, R. H., *J. Met. Club Roy. Coll. Technol.* no. 10, 41 (1958–59).
31. FRENNET, A., AND LIENARD, G., *J. Res. Inst. Catalysis, Hokkaido Univ.* **16**, 115 (1968).
32. HAYWARD, D. O., AND TRAPNELL, B. M. W., "Chemisorption" Plenum, London, 1964.